



Article

The First Inventory of Rock Glaciers in the Zhetysu Alatau: The Aksu and Lepsy River Basins

Azamat Kaldybayev ^{1,2,*}, Nurmakhambet Sydyk ^{1,2}, Alena Yelisseyeva ¹, Aibek Merekeyev ¹, Serik Nurakynov ¹, Kanat Zulpykharov ^{1,2}, Gulnura Issanova ³ and Yaning Chen ⁴

¹ Institute of Ionosphere, 050020 Almaty, Kazakhstan

² Department of Geography and Environmental Sciences, Al-Farabi Kazakh National University, 050040 Almaty, Kazakhstan

³ Research Centre for Ecology and Environment of Central Asia (Almaty), 050060 Almaty, Kazakhstan

⁴ State Key Laboratory of Desert and Oasis Ecology, Xinjiang Institute of Ecology and Geography, Chinese Academy of Sciences, Urumqi 830011, China

* Correspondence: azamat.kaldybayev@gmail.com

Abstract: While rock glaciers (RGs) are widespread in the Zhetysu Alatau mountain range of Tien Shan (Kazakhstan), they have not yet been systematically investigated. In this study, we present the first rock glacier inventory of this region containing 256 rock glaciers with quantitative information about their locations, geomorphic parameters, and downslope velocities, as established using a method that combines SAR interferometry and optical images from Google Earth. Our inventory shows that most of the RGs are talus-derived (61%). The maximum downslope velocity of the active rock glaciers (ARGs) was 252 mm yr⁻¹. The average lower height of rock glaciers in this part of the Zhetysu Alatau was 3036 m above sea level (ASL). The largest area of rock glaciers was located between 2800 and 3400 m ASL and covered almost 86% of the total area. Most rock glaciers had a northern (northern, northeastern, and northwestern) orientation, which indicated the important role of solar insolation in their formation and preservation.

Keywords: rock glacier; inventory; Tien Shan; InSAR; Zhetysu (Dzhungar) Alatau; permafrost



Citation: Kaldybayev, A.; Sydyk, N.; Yelisseyeva, A.; Merekeyev, A.; Nurakynov, S.; Zulpykharov, K.; Issanova, G.; Chen, Y. The First Inventory of Rock Glaciers in the Zhetysu Alatau: The Aksu and Lepsy River Basins. *Remote Sens.* **2023**, *15*, 197. <https://doi.org/10.3390/rs15010197>

Academic Editors: Ulrich Kamp, Dmitry Ganyushkin and Bijeeesh K. Veettil

Received: 11 November 2022

Revised: 24 December 2022

Accepted: 27 December 2022

Published: 30 December 2022



Copyright: © 2022 by the authors. Licensee MDPI, Basel, Switzerland. This article is an open access article distributed under the terms and conditions of the Creative Commons Attribution (CC BY) license (<https://creativecommons.org/licenses/by/4.0/>).

1. Introduction

1.1. Importance of Inventorying Rock Glaciers

There are many options for defining rock glaciers; therefore, different researchers interpret this term differently. Several scientists [1–4] have defined a rock glacier as an accumulated mixture of debris and ice located on a mountain slope that has been deformed under gravity and has formed vicious striking tongue formations that flow up to a kilometer wide and up to several kilometers long. According to Berthling [5], rock glaciers can be determined as “a visible manifestation of cumulative deformation resulting from long-term creep of mixtures of ice and debris in permafrost conditions.” The same definition was used by [6] in their work. It has been reported [7–10] that rock glaciers are reed or lobed landforms on high mountain slopes, usually consisting of a mixture of loose rock fragments and ice.

In this paper, we used the definition presented in the documents of the International Permafrost Association (IPA) [11,12], which define rock glaciers as detrital landforms formed as a result of former or current creep of frozen ground (permafrost), found in a landscape with the following morphology: front (mandatory criterion), lateral margins (mandatory criterion), and possibly a ridged and furrowed surface (optional criterion) (Figure 1). That is, rock glaciers are (or were) landforms that carry debris from an uplift (original zone or root zone) to their front.

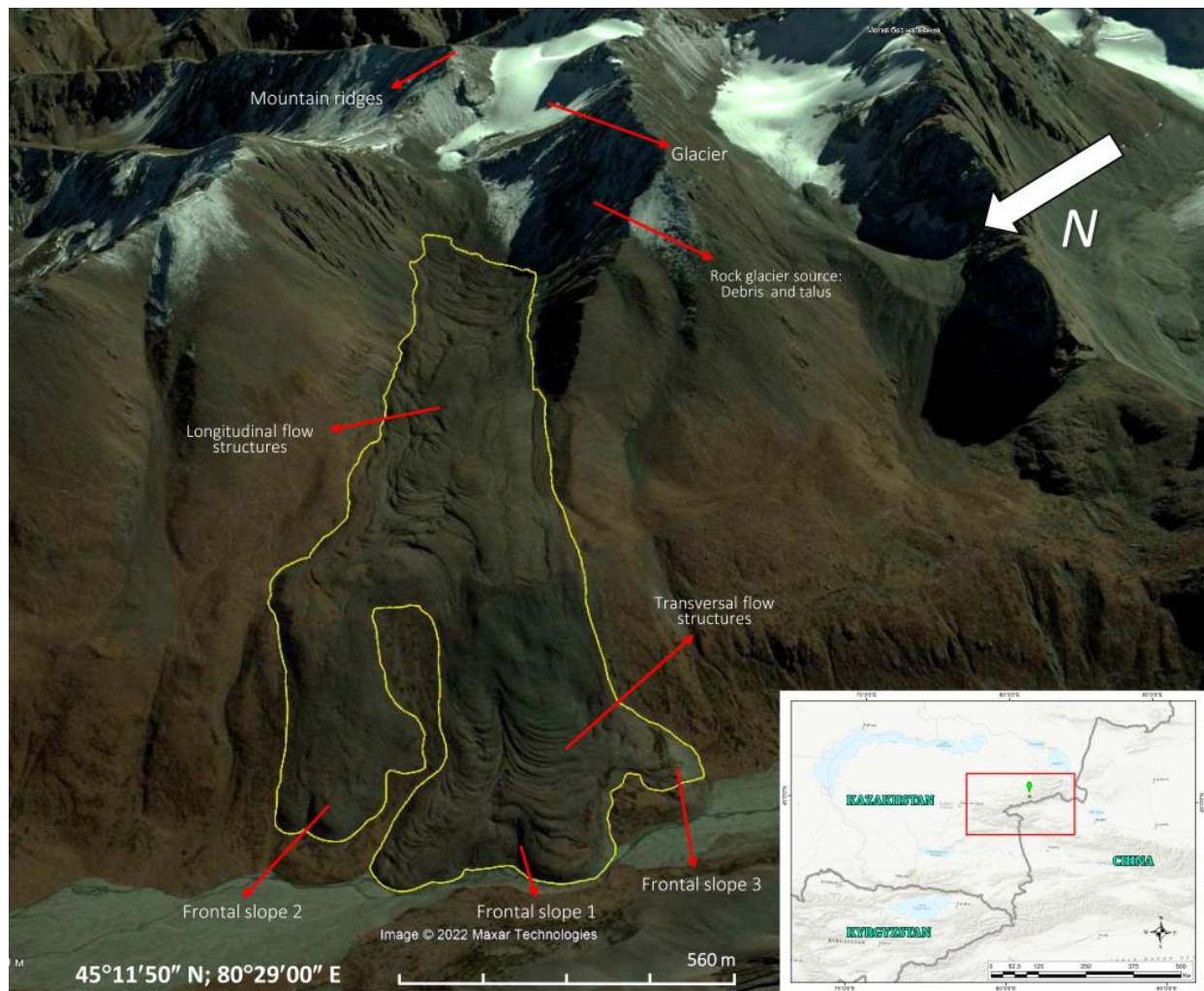


Figure 1. Geomorphology of the rock glacier (RG Nizkomorenniy, Lepsi river basin).

Rock glaciers play an important role in the water balance of high mountain regions [13]. Mountain rock glaciers contain globally significant water stores. Their ability to store fresh water in winter makes them important sources of fresh water in summer for semi-arid and arid regions such as the central Andes and the Sierra Nevada [14–18]. Recent studies have highlighted the importance of rock glaciers as temperature- and climate-tolerant water stores, as well as buffers for hydrological seasonality due to the insulating effect of debris [13,19,20]. Their importance in mountain hydrology is likely to increase in the coming decades due to global glacier retreat [21].

Rock glaciers have geomorphological, climatic, and hydrological significance in alpine periglacial conditions. Rock glaciers can take several thousand years to form and are visible indicators of permafrost that contribute significantly to the mass transport of alpine landforms [22,23]. As such, knowledge of their distribution can provide reliable information on past occurrences of permafrost and associated climatological conditions [24–27]. However, there are cases where subsurface ice can still be found in favorable conditions at much lower altitudes.

1.2. Classification of Rock Glaciers by Their Activity

An active rock glacier is a landform that transports sediment from the root zone to its front. It is characterized by a steep front (steeper than the angle of repose) and possibly by flanks with fresh exposed material at the top [11]. The displacement rate can vary from tens of centimeters to several meters per year [28]. Transitional (intermediate) rock

glaciers have ice in their composition and move at a speed of less than one decimeter per year. Depending on the topographic and/or climatic context, transitional rock glaciers can evolve either into a relict or an active state. A relict rock glacier is a landform that no longer transports sediments from the root zone to its front due to permafrost depletion. In other words, they do not move and do not have ice in their composition. Relic rock glaciers are usually formed at lower elevations than active rock glaciers.

Speed is affected by changes in ground temperature, as well as the presence of moisture, which can speed up or slow down a rock glacier on a ten-year scale [29–32]. Rock glaciers also show strong seasonal fluctuations in surface movement in many cases, with higher velocities in summer and autumn compared to winter and spring [27,33,34].

The IPA Rock Glacier Inventory (RoGI) and Kinematics Action Group, established in 2018 [35], intends to support the development of generally accepted basic concepts and standard guidelines for the inventory of rock glaciers in mountainous permafrost regions [11]. One of the most important elements in standardized RoGI catalogs is kinematic information. Since indirect kinematic information is often inaccurate as it relates to operator interpretations, the result of visual observations of morphological (e.g., fore angle) indicators associated with vegetation [36,37] can be highly unsatisfactory. Recently, more accurate approaches based on remote sensing data (e.g., Sentinel-1 image satellite interferometry) [38] have been developed to characterize rock glacier kinematics on a large scale [16,34,39–41].

In this context, as part of the European Space Agency (ESA) Permafrost Climate Change Initiative (Permafrost_CCI), the so-called CCN2 project (<https://climate.esa.int/en/projects/permafrost/>; last accessed: 10 October 2021)—in line with the basic concepts proposed by the IPA Action Group [11,42]—specific guidance has been developed [28] for the systematic integration of kinematic information into RoGI using InSAR data. Under this framework, workflow is reduced to outlining moving areas and assigning a speed class based on the results of interferometric analyses; attribute information is filled in according to IPA standards.

Rock glaciers are common in Northern Tien Shan, and their descriptions can be found in studies from the beginning of 20th century; moreover, in 1923, researchers took measurements of the rock glacier front [43–46].

It was initially believed that these rock glaciers were mainly of a periglacial origin, but they may also contain sedimentary ice [47,48]. One of the latest studies of rock glaciers in the Zhetysu Alatau region Gorbunov [49] identified about 850 active rock glaciers based on aerial photography at a scale of 1:10,000; the photographs are dated 1969, 1979, and 1984, and they do not specify information about geographical coordinates and topographic parameters. However, descriptions and detailed ground-based geodetic measurements were performed for only one of them—the rock glacier Nizkomorenyy [50]. The altitudinal boundaries of the active rock glaciers are 200–300 m lower in this region than in the relatively well-studied Ile Alatau Range of the Tien Shan mountain system [49].

Other research results are absent for the Zhetysu Alatau region. Our inventory work was started from scratch, and has so far been completed for the Aksu and Lepsy River Basins of the Zhetysu Alatau. Therefore, the main task of our work was to compile an initial digital catalog according to international standards [11,12,28] and evaluate the kinematic performance of rock glaciers in the region.

2. Territory of Interest

The Zhetysu Alatau (or Dzhungar Alatau) is a mountain system stretching from west–southwest to east–northeast along the state border between the Republic of Kazakhstan and the People’s Republic of China. The total area of the Zhetysu mountain system, including the basin of the river Borotala in China, is about 40,000 km² [51]. The Zhetysu mountain system is located mostly in Kazakhstan.

The Ile River is the southern border of this mountain system, while the northern border is the Balkhash Plain and the Alakol Lake and Dzhungar Gates are the northeastern border.

The longitudinal river valleys—Koksu in the west and Borotala in the east—divide the Zhetysu Alatau into two large ridges parallel to each other: the North Central and the South Central.

The length of the North Central Range is about 400 km, and that of the South Range 300 km. The Northern Zhetysu Alatau includes the longest and highest ridge of this mountainous country. Sub-latitudinally, the ridge stretches for 260 km, reaching the highest elevation of 4622 m ASL (Besbakan). The largest spurs of the ridge are Kungei and Tastau.

The Southern Zhetysu Alatau includes the Toksanbay and Bedzhintau ridges, both of which have many spurs. The Muztau mountain range houses the highest peak of the Southern Zhetysu Alatau, which reaches 4370 m ASL. The Southern Zhetysu Alatau also includes the Tyshkantau ridge, as well as the isolated, relatively low Koyandytau, Suat, and Altynnemel ridges with low-mountain spurs [52].

The Zhetysu Alatau is influenced by arctic, polar, and tropical air masses, which undergo significant transformations on their way to the ridges. Arctic air masses come from the north and northwest, from the regions of the Barents and Kara Seas. More often, they come during the early winter period, and their invasions are accompanied by a sharp drop in air temperature.

In the Zhetysu Alatau, the average annual rainfall is 600–800 mm; in the southeast of the ridge, average annual rainfall is 400 mm. In western Dzungaria, the largest annual precipitation in the entire range of altitudes falls in river basins. Chizha Range has the highest precipitation rate (1400–1600 mm) and thus propels moisture-carrying air masses.

The average long-term air temperatures in the lower parts of the glacial zone (at altitudes of 3200–3600 m ASL) during the accumulation period are -8 – -10 °C; in the upper parts (above 4000 m ASL), temperatures drop by up to -14 – -16 °C. The coldest month is January, with temperatures of -17 – -19 °C. The maximum temperatures associated with the intrusions of thermal air from the surrounding deserts reach 13 – 15 °C, and the observed absolute maximum is 25 °C. Thus, the great differences in the absolute heights of the mountain relief of the Zhetysu Alatau and its complex morphology are the cause of a wide variety of climatic conditions. The altitudinal boundary of the permafrost belt in the Dzungarian Alatau coincides approximately with the isohypse of 2500 m ASL; these are 200 m lower than in the Northern Tien Shan [53]. However, unfortunately, the data for this book were collected mainly during 1988.

The average height of the Zhetysu Alatau glaciers is about 3578 m in 2016 and the average maximum and minimum heights are 4545 m and 2869 m, respectively [54–58]. The relative average height of the glaciation zones is lower than in other regions of the Tien Shan. For example, in the central Tien Shan, the average height of the glacier is about 4316 m, respectively, the average maximum and minimum heights are 5112 m and 3707 m [59]. Additionally, in the northern part of the Tien Shan, according to research by Narama and others [60], the average height of glaciers is 3909 m (Ili-Kungöy), the average maximum and minimum heights are 4939 m and 3306 m., respectively.

The Zhetysu Alatau glaciers, as the main source of moraine-derived rock glaciers, have been studied by number of authors. Severskiy and others [61] conducted detailed studies of the ice-cover dynamics for the entire Zhetysu Alatau Range over the period from 1956 to 2011, and they showed that the annual glacier reduction rate was 0.7% in the Aksu–Bien and Lepsy–Baskan river basins. At the same time, they noted that the most intensive reduction rate of the glaciers was observed mainly in the basins of the Southern Zhetysu Alatau, while it was at its lowest in orographic closed basins. In this paper, we considered areas of the Aksu and Lepsi river basins of the Zhetysu Alatau Range (Figure 2).

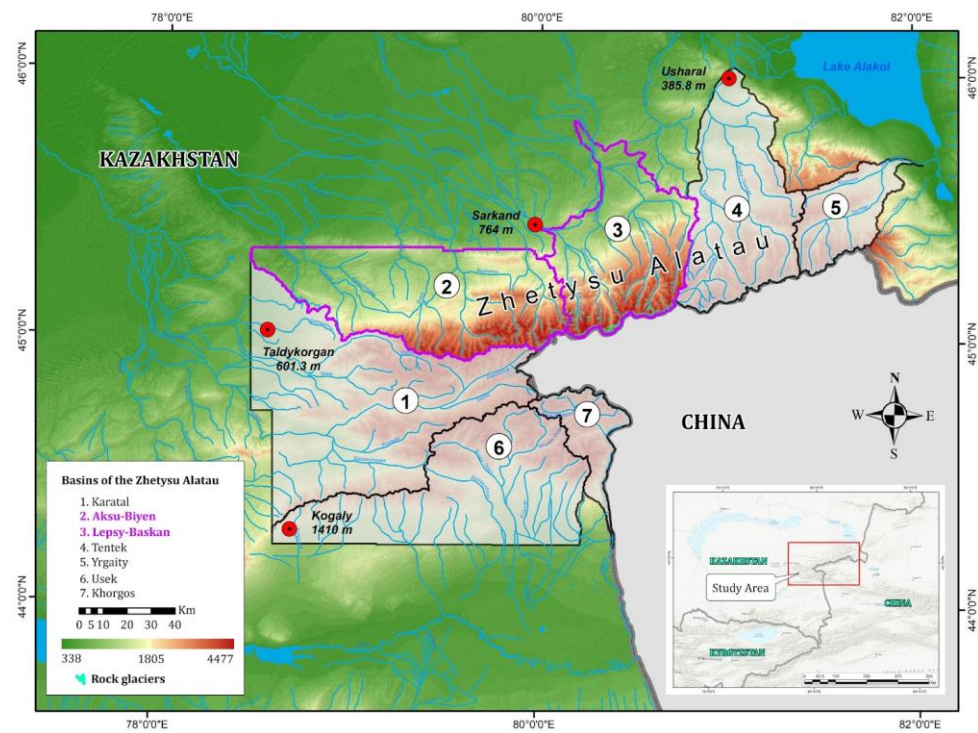


Figure 2. The Zhetysu Alatau basins, including Aksu and Lepsi rivers (purple boundary).

3. Materials and Methods

We used two basic approaches as the main methodology: geomorphologic and kinematic. In this regard, the general workflow for creating an inventory of rock glaciers consists of the following steps: the manual interpretation of the rock glacier contours were based on optical satellite images in the Google Earth environment by visual interpretation of their geomorphological features; then, generate the line-of-sight direction (LOS) surface velocity estimated from Sentinel-1 InSAR data [6,40,62,63], which are described in the IPA and International Centre for Integrated Mountain Development (ICIMOD) manuals. According to the guidelines of the IPA [11,12,42], the systematic inventory procedure for rock glaciers consists of three stages, which are described below and illustrated in Figure 3. This diagram [64] was adapted to the conditions and availability of initial data for the study region.

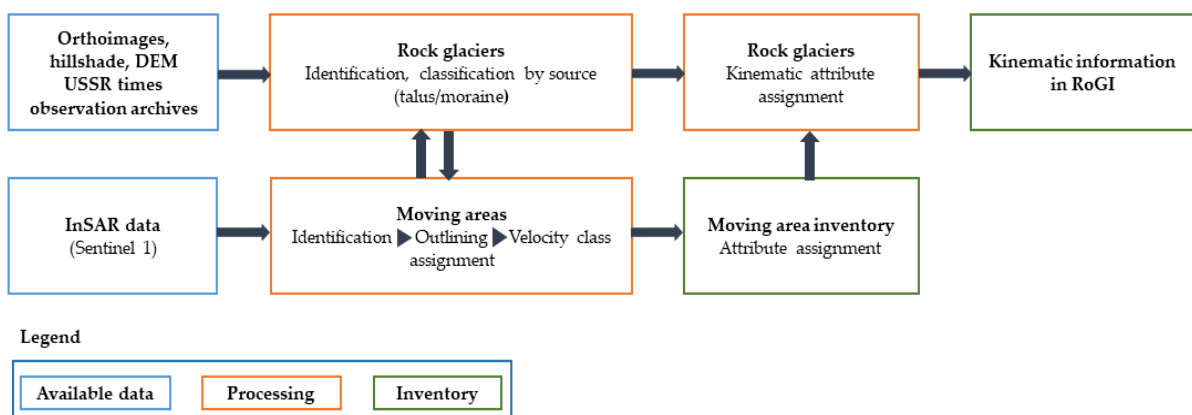


Figure 3. Conceptual diagram of a standardized method for creating a moving area inventory and RoGI, including kinematic information. The analysis is performed in the GIS environment.

3.1. Delineation of Rock Glaciers by Geomorphologic Approach

The geomorphological approach represents visual detection using high-resolution images and DEM-based products. Surface texture and morphometric analyses can also be used for this purpose. This is a classic approach that is complemented by field visits. This makes it possible to produce an exhaustive list of assumed moving and stationary landforms, the distinction of which (activity classes) is primarily based on geomorphological characteristics. Photogrammetry and LiDAR DEM imaging, when available, facilitates the identification of rock glaciers in forested areas.

We inventoried rock glaciers by geomorphological characteristics using high-resolution remote sensing data available on the Google Earth platform according to the methods explained in [65,66] according to the descriptions given in the IPA instructions. Rock glaciers frequently have transverse ridges and furrows, lateral margins, and talus-like fronts due to the deformation of internal ice (see Figure 1). They rarely have the following indicators: crevasses with exposed ice, abundant thermokarst, abundant supraglacial lakes, ice cliffs, supraglacial streams/channels, and a high (over 1 m/yr) subsidence rate. Due to the constant supply of talus or debris, the surface textures of rock glaciers are usually different from the surrounding slopes, and their surface slopes usually have little or no vegetation [40]. Based on these criteria, we visually mapped the landforms in the images correspond to the moving targets in the interferograms and identified the rock glacier. To distinguish the rock glaciers from permafrost and bare ground surface velocity obtained from InSAR was used.

Google Earth data have been applied to a number of research areas [67–73]. Google Earth uses SPOT images or Digital Globe products (e.g., Ikonos and QuickBird) at a resolution that is close to aerial photographs. The images were georeferenced with a DEM based on the Shuttle Radar Topography Mission SRTM data, which have a resolution of 90 m in the study area. In addition, Google Earth supports user-friendly GIS tools that help in building custom databases and exporting data as KML files and converting them to shapefiles for further analysis in the GIS environment [13,74]. Google Earth has previously been used as a platform for rock glacier mapping in British Columbia, the Bolivian Andes, the Hindu Kush Himalaya region, and the Himalayas of Nepal [13,22,74–76]. In the absence of any spectral and spatial information about the images used, quantifying uncertainty into the inventory was difficult. However, in a similar location [74], image fidelity was found to be sufficient for this purpose. Rock glaciers are classified as transitional or active based on their surface velocity. Rock glaciers with unclear surface velocity only fired if the InSAR sensitivity in that area was low, in which case they fired with indeterminate activity. Debris-covered glaciers and rock glaciers are two ends of a continuum [19,77]. Debris-covered glaciers with visible bodies of ice upslope, abundant thermokarst, abundant supraglacial lakes and other visible indicative features listed in IPA guidelines [12] were not included in the rock glacier inventory.

3.2. Identifying Surface Velocity Using SAR Interferometry

Kinematic approach: The differential interferometry method detects the movements of the Earth's surface using the phase differences between two radar images taken at different times [78]. Since the phases of the differential interferogram were wrapped between $-\pi$ and π , one phase cycle corresponded to half a wavelength (e.g., 2.8 cm for C-band [16]) of surface displacements along the direction of the radar sighting beam [78].

In our paper, images from the Sentinel-1 satellites of the SLC level were used; these are a freely available Alaska Satellite Facility (<https://asf.alaska.edu/> (accessed on 26 April 2022)) resource, and they make it possible to select a stack of images for multi-pass processing. The IW mode has a resolution of 20 m in azimuth and 5 m in range. The selection of radar images was based on the following criteria: The survey period was 5 years from 8 August 2017 to 28 September 2021 with a seasonal restriction (only 2 months of August and September were selected); the total number of images was 25 for ascending and 26 for descending orbits. To achieve high interferometric coherence, a maximum time base

of 48 days was chosen. According to the specified criteria, 49 interferometric pairs were built for images in the upward survey geometry and 52 pairs for the downward survey. Basic survey parameters: ascending orbit—path 158, frame 142; descending orbit—path 136, frame 441; IW survey mode.

We chose only two months of observations because of minimal snow cover occurring only during August and September. This is a serious limitation in achieving sufficient coherence between surveys [79]. The image series was processed using the intermitted SBAS method [80] or discrete SBAS, where the timeline was set as hard and the whole stack started with broken links (because only a few months were included in the processing). The discrete SBAS method interpolates the time periods when pixel coherence falls below the selected coherence threshold on some interferograms, and also results in a significant improvement in spatial coverage compared to the original SBAS algorithm for partially vegetated study areas [81,82].

Interferometric processing was performed using ENVI software with an additional SARscape multimodule (©Sarmap SA, 2001–2020). Stack processing was performed in the standard settings of the Sentinel TOPSAR mode and according to the pipeline (processing steps) in the SBAS module.

Then, the values of displacement velocities from LOS units were converted into values of vertical velocities in millimeters. The resulting raster surfaces of vertical velocities were cut from a vector file with geomorphological contours of rock glaciers; from the stripped values, the maximum and minimum speed indicators were extracted into the attribute information. Raster surfaces, prior to cutting geomorphological contours, also underwent an additional procedure for evaluating all selected moving areas in order to validate and cut-off moving areas whose kinematic nature was associated with slope processes and other phenomena. When re-comparing the geomorphological contours of rock glaciers and the raster of motion velocities, several objects were refined and supplemented. To move into the kinematic categories, seven classes were created (<1, 1, 1–10, 10, 10–100, 100, and >100 cm/yr). The choice of kinematic classes was made according to the proposals of the international working group [42].

Where the calculated speed was close to the upper limit of the speed class, the ARG was assigned to that faster class because the one-dimensional line-of-sight measurement provided by radar interferometry represents only one motion component, and thus typically underestimates the actual three-dimensional surface motion [6]. The same was enacted with the natural temporal variations in surface displacement rates; i.e., if two or more classes were present during the observation time interval, the highest displacement speed was used to determine the speed class.

Finally, we derived the topographic/geometric parameters using Spatial Analyst tools in the GIS environment. Height information was determined from the SRTM DEM. Our inventory lists the geographical locations (including longitude, latitude, and altitude), the geomorphic attributes (including area, length, aspect and PISR), and the surface velocity of each rock glacier. Then, we compiled a spreadsheet to summarize the characteristics and calculate the total statistics.

4. Results

For the first time since the 1990s, rock glacier identification and inventorization work was carried out in the Lepsy and Aksu River basins of the Zhetysay Alatau, and their detailed digital catalog was compiled in accordance with international standards [11,83].

A total of 256 rock glaciers were identified, with a total area of more than 28.5 km² and an average lowest boundary at 3036 m ASL; the rock glaciers were 0.11 km² by average size. The largest rock glacier was 1.53 km² by size, while the smallest rock glacier had an area of about 0.004 km². According to the kinematic categorization for speed assessment, we found that active rock glaciers counted for 204 units; 47 of their total number were included in the transitional category and 5 were relics.

4.1. Type of Rock Glaciers Origin

Talus-derived types of rock glaciers were more numerous than those of moraine origin. About 61%, or 156 rock glaciers, were formed from talus in the Lepsy and Aksu River basins, while the remaining 39% (100 glaciers) were formed from moraines (Figure 4). Several rock glaciers were also found in the study area with several episodes of activity, where newer lobes dominated older ones. Complex rock glaciers with more than one root zone are most common in the study area. Figure 5 shows examples of rock glacier origin types in two basins of the Zhetysu Alatau Range.

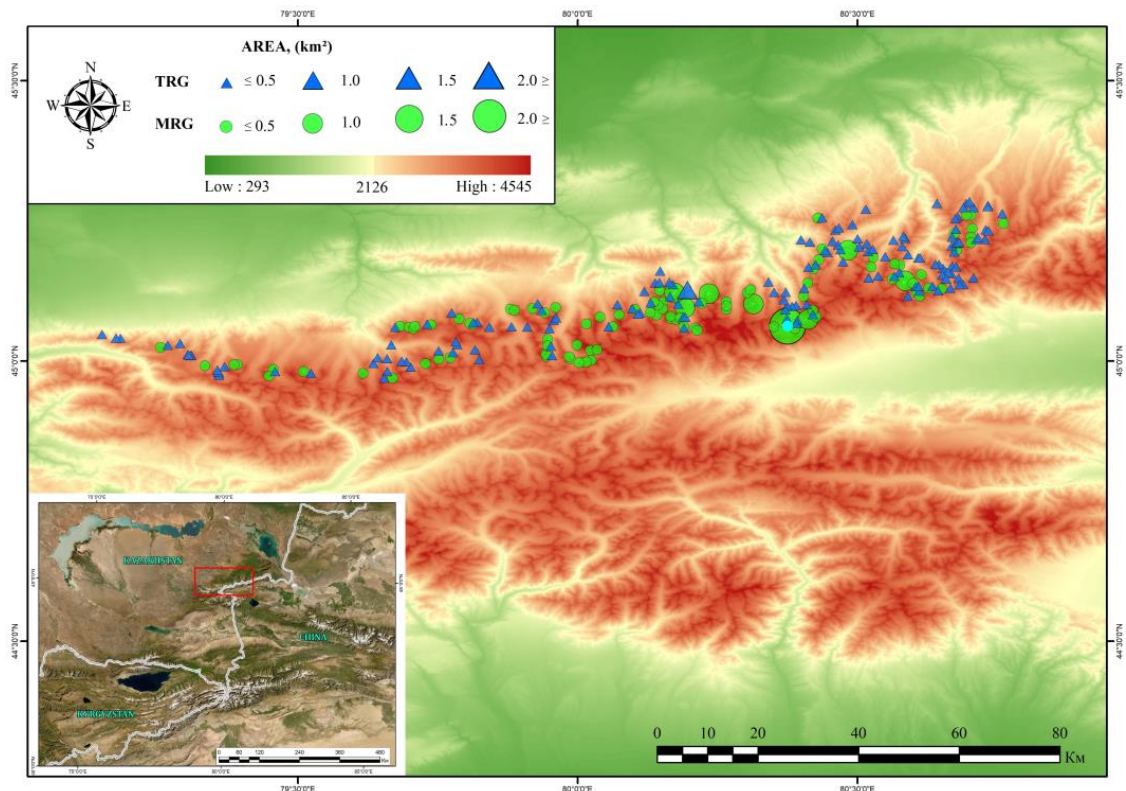


Figure 4. Topographic map of the Zhetysu Alatau. Green circles and blue triangles represent Moraine rock glaciers (MRG) and Talus rock glaciers (TRG), respectively. The size of the circle and triangle represents the size of the rock glacier.

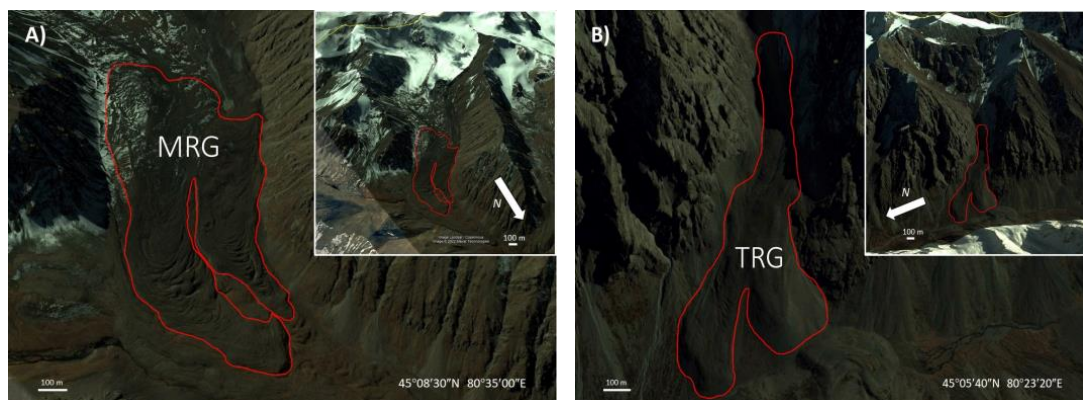


Figure 5. Google Earth images of (A) typical moraine rock glacier (MRG) and (B) talus rock glacier (TRG). The insets show the topographic and morphological features surrounding the same rock glaciers.

According to the results of the analysis of the topographic/geometric parameters, the north-facing slopes, which have lower solar radiation, are more favorable for the formation of rock glaciers than the south-facing slopes. The number of inventoried rock glaciers in this study can be considered a conservative estimation due to limitations in remote sensing data and human factors. As such, more rock glaciers in this area cannot be ruled out. Table 1 lists the main characteristics of the rock glaciers obtained in our analysis.

Table 1. Main characteristics of rock glaciers located in the Aksu and Lepsy River basins.

	Area (km ²)	Slope (°)	Altitude (m)	Pot. Radiation (W/m ²)	Minimum Altitude at the Front (m)	Maximum Altitude of Rock Glaciers (m)
Mean	0.11	16.9	3101	1,025,519	3036	3165
Std deviation	0.16	5.0	205	76,791	212	199
Minimum	0.004	7.7	2384	836,379	2384	2614
Maximum	1.53	42.0	3723	1,234,567	3640	3723

4.2. Surface Velocity Evaluation

Quantitative analysis of the distribution of identified rock glaciers showed the following distribution over the combined watersheds of the Aksu and Lepsy Rivers. Thus, 102 RGs were allocated for the Aksu basin and 154 RGs for the Lepsy basin. Depending on topographic factors (topography, slope, size, and amount of ice in the composition), rock glaciers move differently, even if they are located close to each other. According to the manuals [64,83] and research [6], when calculating the velocity, in the case of different speed indicators on the body of one rock glacier, we took the maximum value. In Figures 6 and 7, one circle represents one individual rock glacier with its maximum velocity.

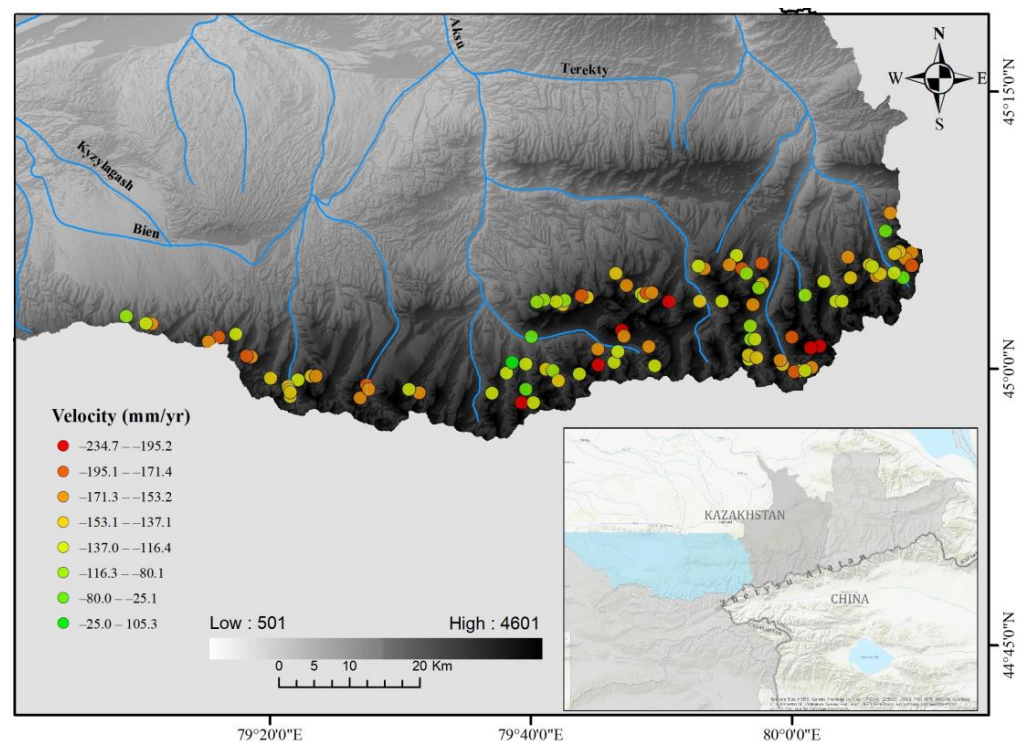


Figure 6. Displacement rates of rock glaciers in the integrated Aksu catchment area.

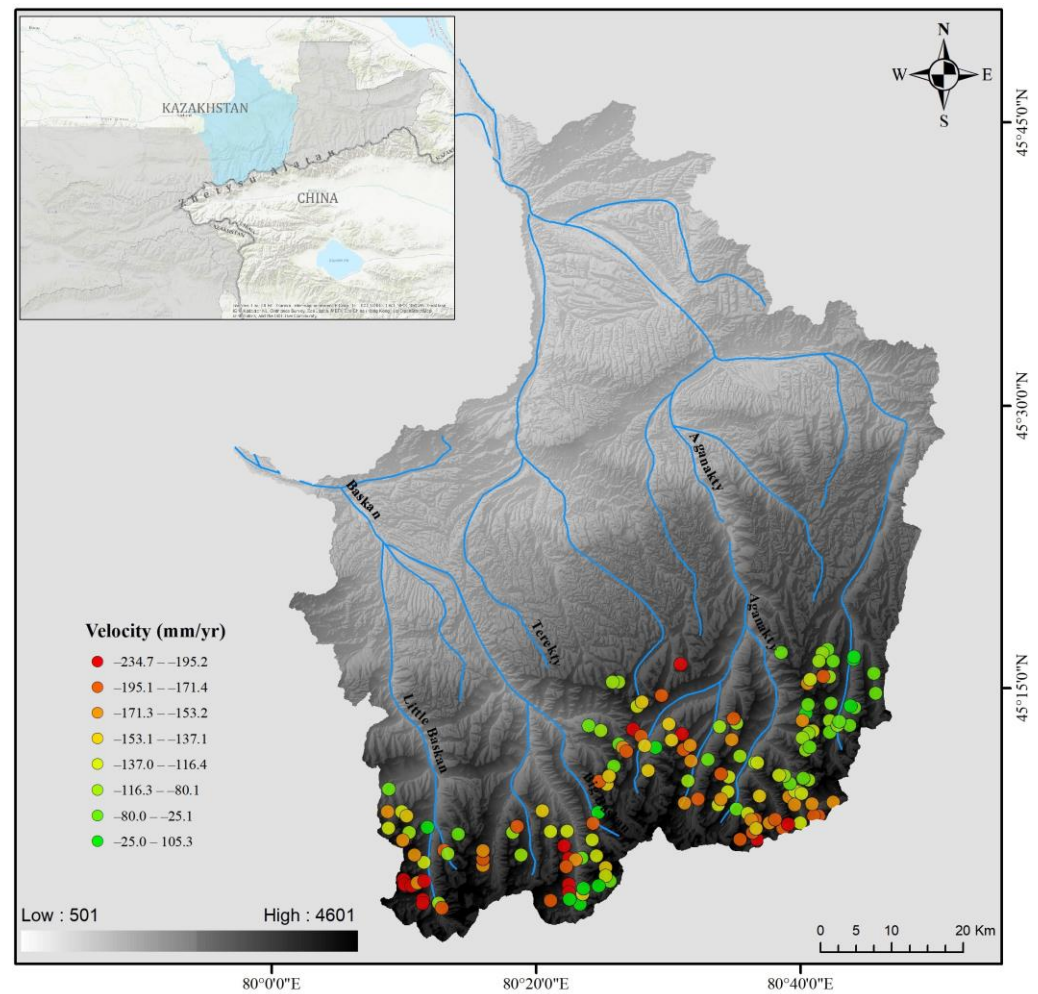


Figure 7. Rock glaciers inventory results for the integrated Lepsy catchment area.

4.2.1. Aksu River Basin

In the Aksu River basin, 93 active rock glaciers were identified, with a displacement rate of up to 240 mm yr^{-1} (Figure 6); eight units fell into the transitional category and one was classified as a relic. The lower elevation mark at which active rock glaciers are located in the basin is 3100 m ASL and the maximum value is 3700 m ASL.

4.2.2. Lepsy River Basin

In the Lepsy River basin, 154 rock glaciers were identified, of which 111 units were active: 39 in the transitional category and 4 in the relict category. The displacement rate in the analyzed basin was also -252 mm yr^{-1} (Figure 7). The lower and upper heights of the location of active rock glaciers ranged from 2600 m ASL to 3720 m ASL.

Velocity field distribution analysis made it possible to identify several groups of rock glaciers with a similar pattern of velocity distribution over the glacier body (Figure 8):

- The first type—the main distribution of moving areas in the middle of the rock glacier body;
- The second type—the location of the moving areas closer to the forehead of the rock glacier;
- The third type is a complex distribution of moving sections in several areas in same glacier body.

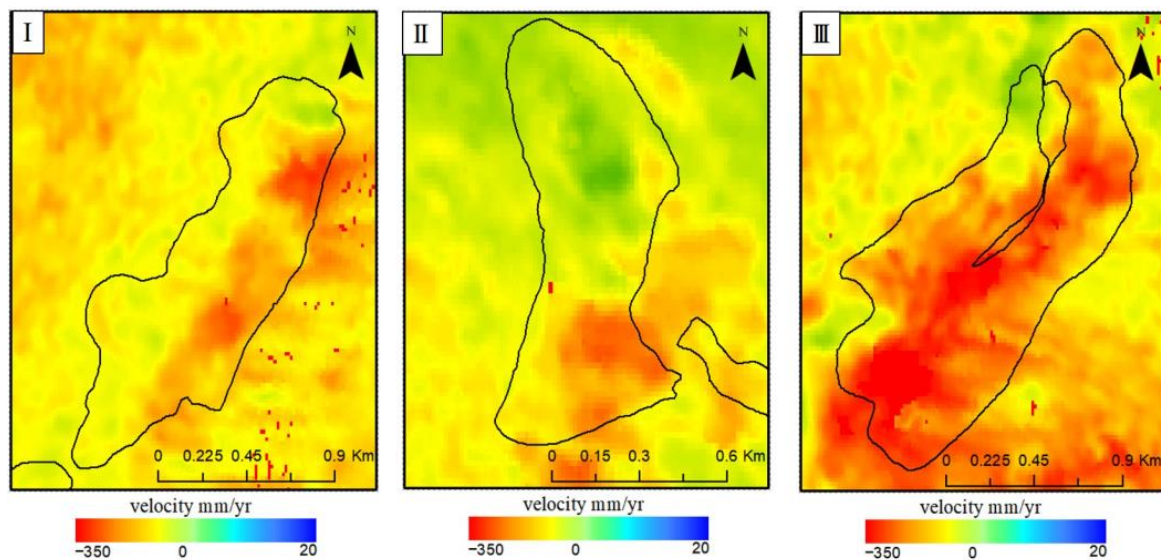


Figure 8. Examples of displacement fields by types of velocity distribution (type I—moving area in the middle, type II—forehead moving area, type III—several moving areas).

A more detailed analysis of velocity distribution types will be carried out in the next part of the work with a scaling of the study area (the entire Zhetysu Alatau).

4.3. Additional Geomorphological Features

4.3.1. Aspect

About 54% of the total area (or 15.4 km²) of rock glaciers was located on slopes with northern exposure: 17% in the northern, more than 20% in the northeastern, and almost 17% in the northwestern exposures. On slopes with western and eastern exposures, 13% and 17% of the total area of rock glaciers were formed, respectively. Only 16% of rock glaciers, covering 4.5 km² of the area, were formed on slopes with southern exposure, including on the slopes of southeastern exposure (SE), where 7% of rock glaciers were observed; in the southwestern exposure (SW), 5% were formed, while only 4% were formed in the southern (S) exposure (Figure 9a,b).

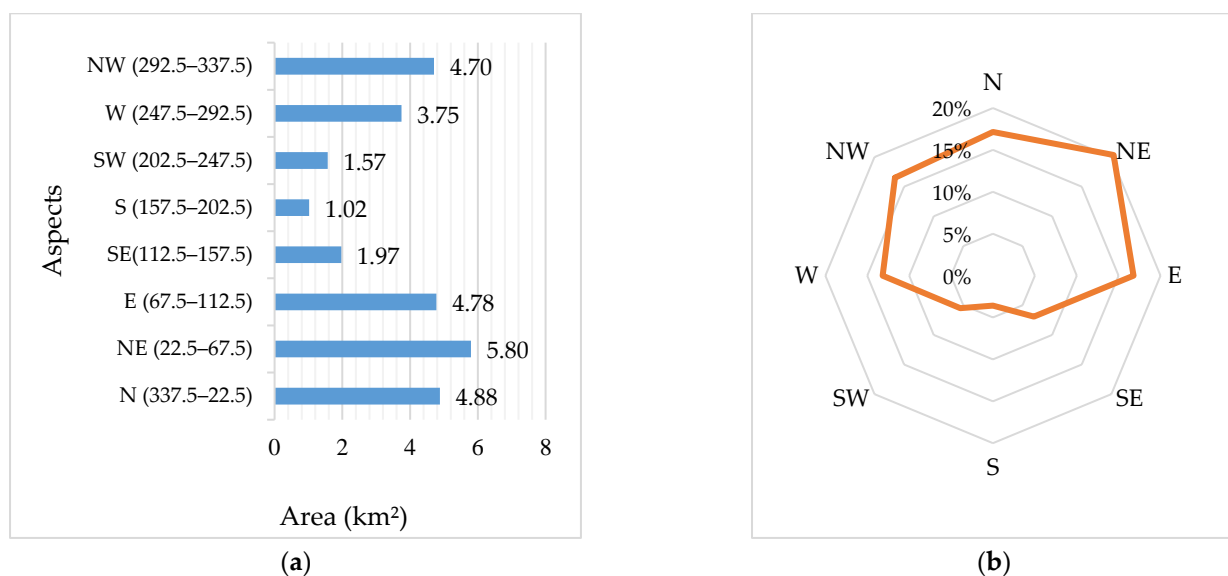
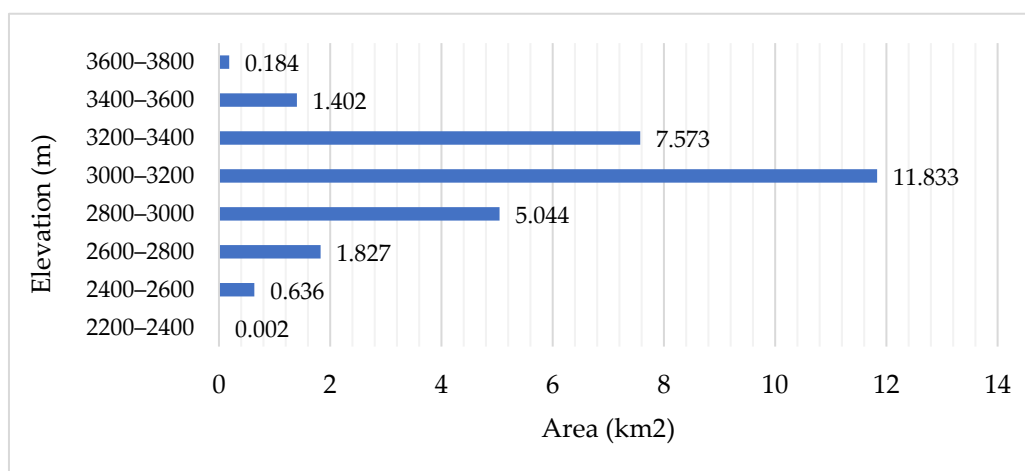


Figure 9. Distribution of rock glaciers by aspect: (a) area ratio (km²) per aspect; (b) percentage of area per aspect.

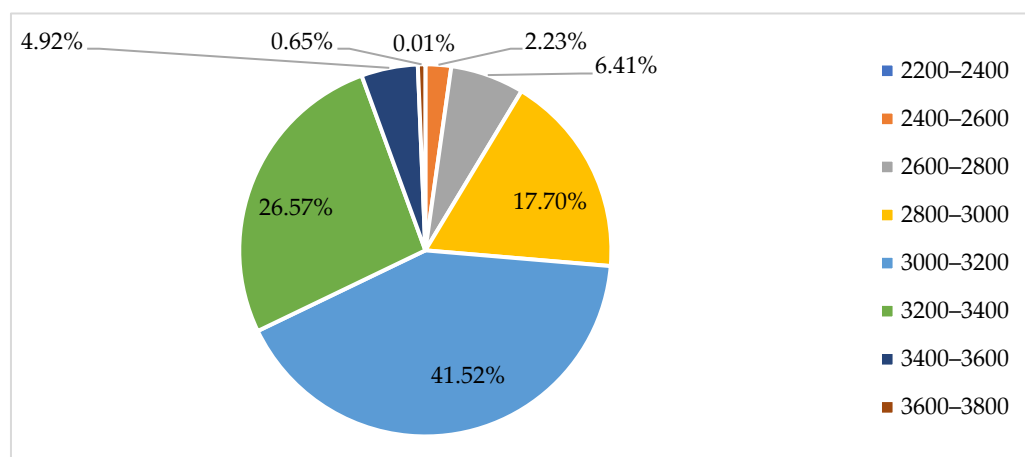
The overall analysis showed that the rock glaciers developed at lower elevations in the slopes of northern aspects and at higher elevations in southern aspects. Significant variability was observed in the aspect distribution of the rock glacier area. The northeast (NE) slopes have a large area of rock glacier, followed by the north (N) and east (E) slopes. In total, more than 5.8 km² of the rock glacier area is located on the northeastern slopes (Figure 9a).

4.3.2. Height Distribution

The largest area of rock glaciers was 24.5 km² and was located between 2800 and 3400 m ASL. This is almost 86% of the total area of the inventoried rock glaciers (Figure 10a,b). Of these, 11.83 km², or 41.5%, of the total area lies within altitudes of 3000–3200 m ASL. The smallest concentration is located between 2200 and 2400 m ASL and 3600 and 3800 m ASL, where glacier amounts are less than 1% in total.



(a)



(b)

Figure 10. Distribution of rock glaciers by height: (a) ratio of area (km²) to height; (b) percentage of area per height.

4.3.3. Accuracy of Evaluation

Accuracy was assessed by two operators by isolating the boundaries of three active rock glaciers once each day over three days (Figure 11). All three rock glaciers were of moraine origin.

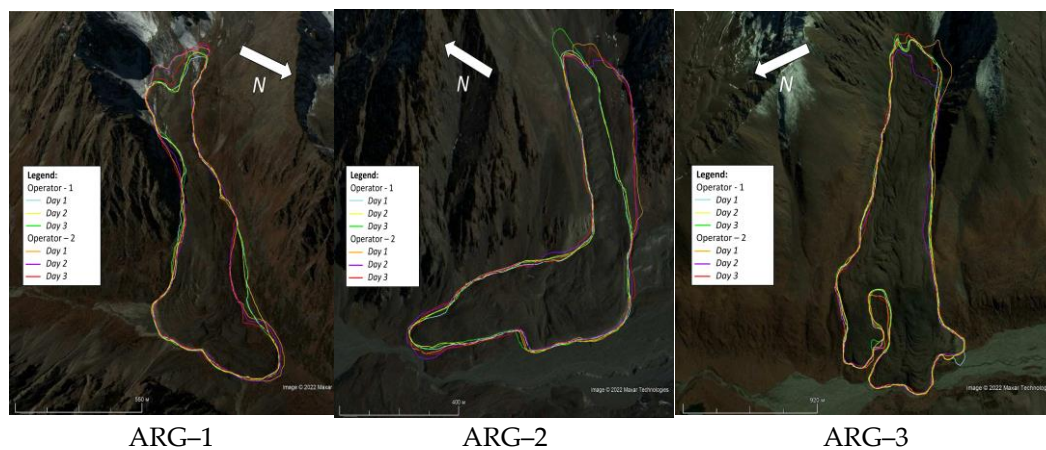


Figure 11. Polygonal outlines of rock glaciers.

During mapping, the fronts of the main tongues were plotted on the map with small differences, and the minimum height of each ARG remained almost unchanged. Rooting zones demonstrated higher variability, which significantly affected maximum height variability (differences in the height of the root zone between two operators: 1-ARG—14 m, 2-ARG—35 m, and 3-ARG—8 m). The sides of the third ARG remained identical for both operators during all three days, while opinions were divided regarding the first and second ARGs. One operator singled out, in the main, the most obvious creeping beats. The other also included scree cones. For ARG-3, the average area for the first operator was 0.58 km², for the second—0.598 km², and for ARG-2—0.198 km² and 0.24 km², respectively (Table 2).

Table 2. The results of the evaluation of accuracy by two operators.

Operator 1			Mean Area (km ²)	Standard Deviation	
	Day-1 (km ²)	Day-2 (km ²)			
Rock glacier-1	0.572916	0.586109	0.582255	0.580426	0.005539008
Rock glacier-2	0.194221	0.198028	0.202213	0.198154	0.003263937
Rock glacier-3	0.906863	0.911821	0.913899	0.910861	0.002951556
Operator 2			Mean Area (km ²)	Standard Deviation	
	Day-1 (km ²)	Day-2 (km ²)			
Rock glacier-1	0.615497	0.601093	0.577631	0.598073667	0.015605464
Rock glacier-2	0.240758	0.239961	0.239547	0.240088667	0.000502563
Rock glacier-3	0.963554	0.888456	0.917465	0.923158333	0.030921815

5. Discussion

In our inventory, 256 rock glaciers were identified in the Aksu and Lepsy River basins (northern Zhetysu Alatau). This inventory of the selected basins made it possible to create a novel digital database on the available rock glaciers in the region, develop cataloging methods according to international standards, and study the features of the region. Based on the experience we gained, even more work is underway to scale the inventory to the entire Zhetysu Alatau region.

Of the main features of rock glacier formation conditions, it is worth noting that northern slopes receiving a lower PISR may represent the most favorable conditions for rock glacier formation, even at lower elevations.

Additionally, glaciers, as the main source of rock glaciers of moraine origin, are rapidly decreasing in size. According to the authors [61], the rate of annual glacier reduction in

the Aksu–Bien and Lepsy–Baskan River basins for the period from 1956 to 2011 is 0.7%. According to Kaldybayev et al. [84], for the period of 2001–2016, Aksu–Bien and Lepsy–Baskan shrank in glacier area by $1.2\% \text{ a}^{-1}$ and $1\% \text{ a}^{-1}$, respectively. In the future, this accelerated shrinkage rate may lead to the appearance of more rock glaciers of moraine origin in the region. It is widely accepted, and many scientists believe, that glaciers with less favorable climatic conditions turn into rock glaciers [19].

The glacier area of the region was obtained from Kaldybayev et al. [84]. The ratio between the area of rock glaciers and the area of glaciers (Figure 12) was significantly higher for the Lepsy basin than for the Aksu basin. This ratio can be considered an indicator of the predominance of glacial and periglacial activity in the region. It can be concluded that periglacial activity in the Lepsy basin prevailed over glacial activity. However, this analysis was simply an attempt to understand the relationship and should be treated with caution due to the lack of comprehensive field observations and validations.

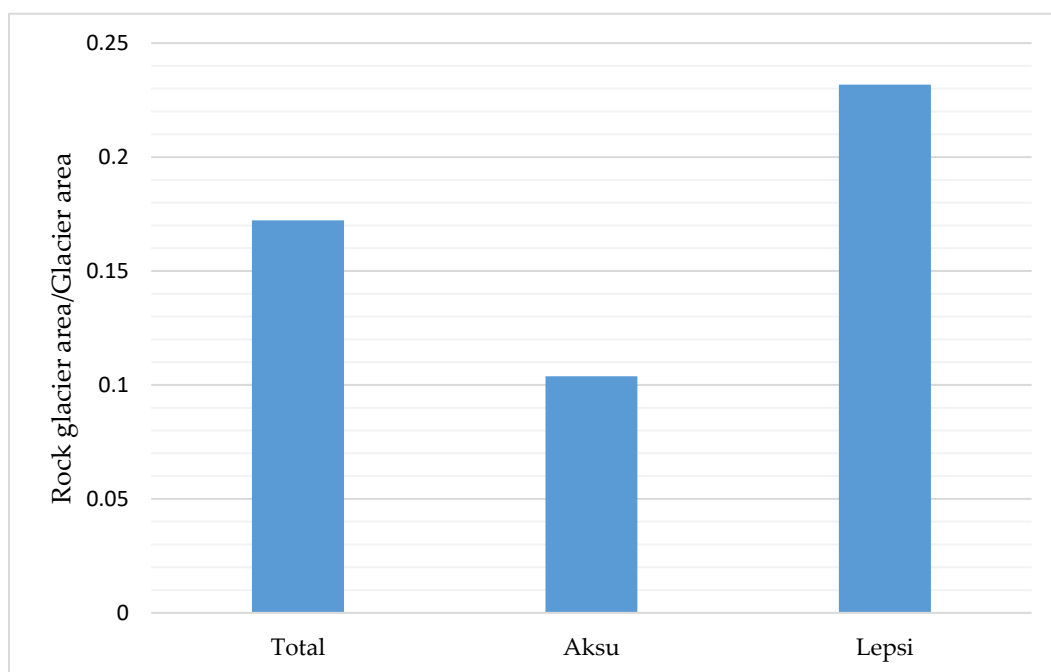


Figure 12. Distribution of the ratio between the area of the rock glacier and total glacier area.

5.1. InSAR Technology Ambiguities

In terms of kinematic-information-collection methods, InSAR time series analysis has great potential for monitoring low-amplitude movement velocities, but this method is not without significant limitations.

The main limitations that arise when calculating displacements using radar interferometry methods are the following: (a) The lack of calculation of displacements measured on moving sections, and the slope displacement projection calculation provides information on displacements in 3D projection; it is worth noting that the magnitudes of the displacements of moving segments on the northern and southern sides are calculated less accurately, even when processing data from the ascending and descending orbits of the satellite; and (b) estimating low-speed moving sections (displacement rates less than 3 cm per year) is insufficient since interferograms with a long timeline contain too much noise, while slow-current displacements are better distinguished by pairs with a large time interval.

The problem of InSAR sensitivity is well known and it causes many issues, especially for landforms with a very low offset. Projecting the LOS offset onto the intended direction of travel (i.e., along the steepest slope) does indeed provide more representative results [85], but the rates are probably still somewhat underestimated. Rock glaciers in areas with poor

InSAR sensitivity are included in the inventory even if their line-of-sight velocity is <1 cm/yr for this reason. Their activity is classified as “undefined”.

5.2. Comparison with Previous Studies of Tien Shan Rock Glaciers

Previous studies of rock glaciers in the Eastern Tien Shan are limited. According to Gorbunov and Titkov [48] active rock glaciers in the Zhetysu Alatau are confined to the zone between 2300 and 3500 m, whereas relict rock glaciers occur down to 2100 m. The bulk of the active near-glacier (moraine-derived) rock glaciers are concentrated within the elevational range of 3000–3200 m, whereas the bulk of the active near-slope (talus derived) rock glaciers are found between 2900 and 3100 m a.s.l. The belt of rock glaciers is 200–300 m lower than in the Northern Tien Shan mountains corresponding to its more northerly latitude [49]. These findings are generally consistent with our inventory. For the sections of the two basins analyzed in our work, the following altitude ranges were identified from 2600 m ASL to 3720 m ASL, which means an increase in the lower limits of the placement of rock glaciers by 300 m higher and an increase in the upper limits by 220 m. The highest surface velocity was found at altitudes of 3000–3400 m ASL (Figure 13). Most likely, this is due to the fact that 68% of the total area of the inventoried rock glaciers is located in this interval.

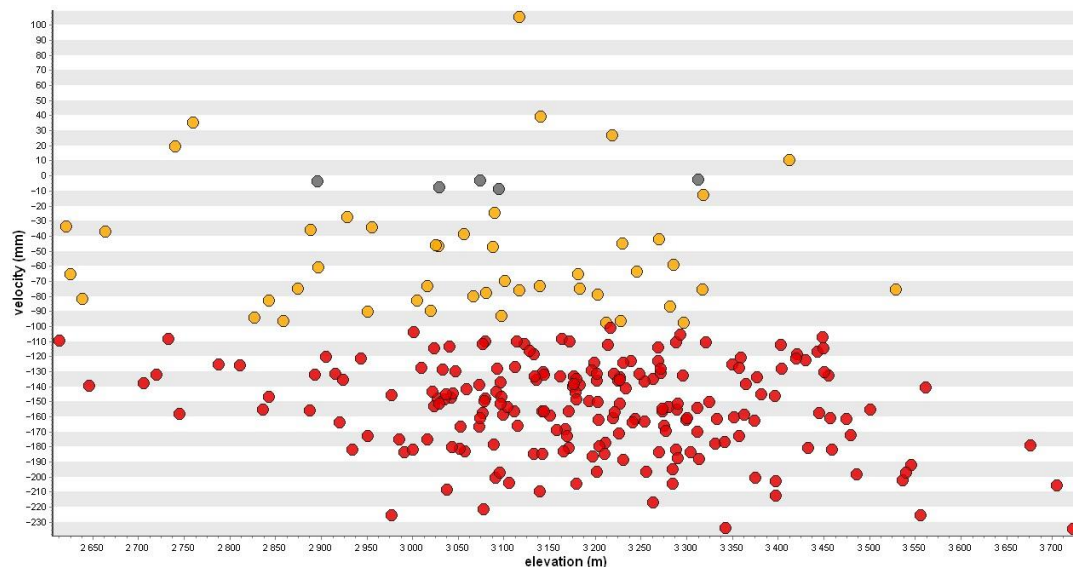


Figure 13. The distribution of the kinematic activity of rock glaciers by height.

The mean size of rock glacier in the Northern Tien Shan is 0.27 km^2 [6]. The highest rooting zone of a rock glacier is situated above 4000 m and the mean elevation is 3480 m. Wang [40] compiled an inventory of active rock glaciers for the Boro-Khoro area (Eastern Tien Shan). Despite the more northern location of the Zhetysu Alatau than the Boro-Khoro ridge, the average PISR value for the slopes of the northern and southern exposures is higher by $1.04 \times 10^5 \text{ W m}^{-2}$ and $1.14 \times 10^5 \text{ W m}^{-2}$, respectively. For both ranges, north-facing slopes are more favorable for rock glacier formation than south-facing slopes. The detected displacement rate in the study region reaches 240 mm yr^{-1} , which is several times less than in Boro-Khoro where, according to researchers, the rates reach 114 cm yr^{-1} . The average area of a rock glacier in the basins of the Aksu and Lepsy Rivers was 0.11 km^2 , while it was 0.35 km^2 on the Boro-Khoro ridge [40]. Additionally, the ratio of types of rock glaciers of talus and moraine origins is 61% and 39%, respectively, while in Boro-Khoro, the ratios are 31% and 69%, respectively.

5.3. Building a Digital Data Catalog That Meets International Standards

For the entire period of observations of rock glaciers in the Zhetysu Alatau, no practical catalog was developed; there were only oral reports from researchers and some field observations of individual rock glaciers. In [53], the author claims that there are at least 850 active rock glaciers in the entire Zhetysu Alatau, while no specific works, inventories, or catalogs have been found in the archives. In our work, for the first time, we have digitalized rock glaciers in the combined watersheds of the Aksu and Lepsy Rivers of the Zhetysu Alatau and compiled a catalog.

However, at the same time, the most studied rock glacier of Central Asia is located in Zhetysu Alatau, which is Nizkomorenniy (Figures 1 and 14). The first cycles of observations on it were started in 1948 by Palgov N.N. [50] and continued until the 1990s. The formation of the rock glacier is associated with the glacier located above, from which the moraine broke off and began to move down the slope with a steepness of 15 degrees, acquiring the form of a rock glacier. The steepness of the frontal ledge is 40–45°. For 34 years (observation periods 1949–1953–1959–1964–1970–1982), the module of the surface velocity of the rock glacier was 0.17 m/year, the maximum was 0.35 m/year, and the total value of its movement was 8.91 m [86].

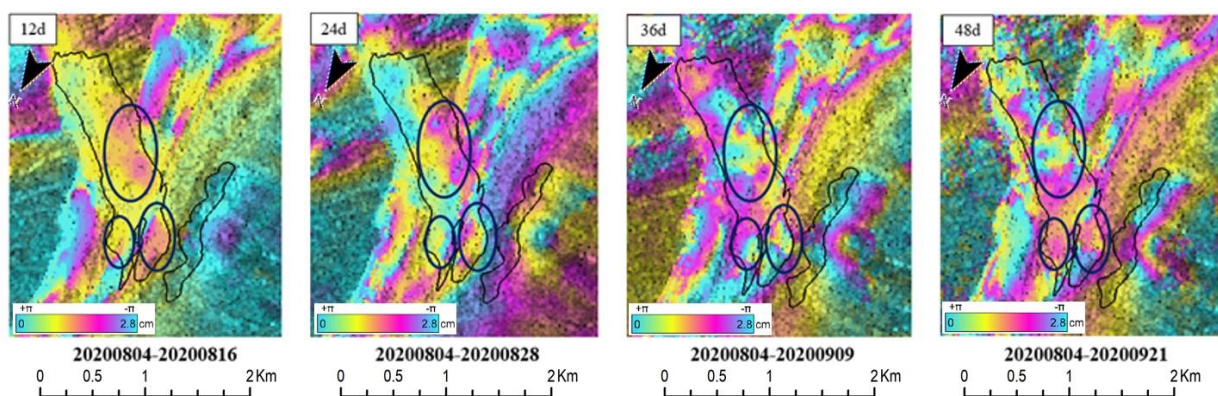


Figure 14. An example of differential interferogram series for the rock glacier—Nizkomorenniy.

In the above series of differential interferograms (Figure 14) for the Nizkomorenniy rock glacier, three areas of movement are clearly distinguished: in the central part of the rock glacier, significant changes in the movement field are noted over 48 days; motion zones are also noted on two frontal slopes of the rock glacier. It should be noted that the two main frontal slopes move with different signs of movement: the first actively gives off mass, while the second one accumulates mass. It bears emphasis, that the described rock glacier has a history of observations of about 70 years and still retains its activity. This glacier has an annual surface velocity rate of $-45--250 \text{ mm yr}^{-1}$ (these values are taken from the surface velocity map by the SBAS method for the 2017–2021 period).

6. Conclusions

This study provided the first comprehensive up-to-date documentation on the characteristics of rock glaciers in the Aksu and Lepsy River basins of the Zhetysu Alatau.

A total of 256 active rock glaciers covering an estimated area of 28.5 km² were inventoried and mapped by combining the use of SAR interferometry and optical imagery from Google Earth.

The average lower height of rock glaciers in this part of the Zhetysu Alatau was 3036 m ASL. About 39% of rock glaciers were of moraine origin, and 61% of them were talus-related. The largest area of rock glaciers was located between 2800 and 3400 m ASL and covered 24.5 km²; this was almost 86% of the total area of the inventoried rock glaciers.

Most rock glaciers had a northern (northern, northeastern, or northwestern) orientation, which indicated the important role of solar insolation in their formation and

preservation. Slopes with lower PISR favored the development of rock glaciers. The height of rock glaciers generally increased from east to west and decreased from south to north, indicating the effect of latitude and longitude on rock glacier location by height.

We also conducted a detailed study of differential interferograms with different time bases to map the surface flow of the Nizkomoreny rock glacier. We found two fast-moving branches in the lower part (frontal slope) of the rock glacier, and a flow zone in the central part of the rock glacier was also relatively active. More importantly, we saw active areas of multidirectional movement throughout the body of the rock glacier.

This inventory has provided a baseline dataset for further studies of rock glaciers as a reservoir, as well as for studying permafrost for slope instability, water resources, and greenhouse gas emissions. The successful application of the proposed method in the Zhetysu Alatau demonstrates that this approach can be applied to other high mountain regions of the world, thereby helping to fill gaps in our knowledge of mountain glaciers on a global scale. This new knowledge will be useful in inferring the distribution of alpine permafrost in high mountains.

Author Contributions: Conceptualization, A.K. and Y.C.; methodology, A.K., N.S. and A.Y.; software, A.Y., N.S. and A.M.; validation, S.N.; investigation, A.K. and N.S.; data curation, A.K. and K.Z.; writing—original draft preparation, N.S. and A.Y.; writing—review and editing, A.K., N.S., A.Y. and G.I.; visualization K.Z.; supervision, A.K. and Y.C.; project administration, A.K.; funding acquisition, A.K. and S.N. All authors have read and agreed to the published version of the manuscript.

Funding: This research has been funded by the Science Committee of the Ministry of Education and Science of the Republic of Kazakhstan within the framework of the projects: AP08856470, AP14872134, AP09058619 and supported by the Postdoctoral Fellowship provided by Al-Farabi Kazakh National University. The APC was funded by the project budget.

Data Availability Statement: Sentinel-1 Single Look Complex images used in this study can be downloaded from the Alaska Satellite Facility at <https://asf.alaska.edu> (accessed on 26 April 2022). Shuttle Radar Topography Mission (SRTM) 90m DEM used in this study can be downloaded from CGIARCSI consortium for spatial information at <https://cgiarcsi.community/> (accessed on 24 April 2022). High-resolution optical images with 3D representation used in this study are available in the program Google Earth.

Acknowledgments: We are grateful to the providers of free data for this study: European Space Agency (ESA)/European Commission (EC) Copernicus, Alaska Satellite Facility (ASF), United States Geological Survey (USGS) and others.

Conflicts of Interest: The authors declare no conflict of interest.

References

1. Capps, S.R. Rock Glaciers in Alaska. *J. Geol.* **1910**, *18*, 359–375. [[CrossRef](#)]
2. Haeberli, W. Creep of Mountain Permafrost: Internal Structure and Flow of Alpine Rock Glaciers. *Mitteilungen der Versuchsanstalt für Wasserbau, Hydrologie und Glaziologie an der Eidgenössischen Technischen Hochschule Zürich*, (77). 1985. Available online: <https://ethz.ch/content/dam/ethz/special-interest/baug/vaw/vaw-dam/documents/das-institut/mitteilungen/1980-1989/077.pdf> (accessed on 29 December 2022).
3. Martin, H.E.; Whalley, W.B. Rock Glaciers: Part 1: Rock Glacier Morphology: Classification and Distribution. *Prog. Phys. Geogr.* **1987**, *11*, 260–282. [[CrossRef](#)]
4. Barsch, D. Rockglaciers: Indicators for the Present and Former Geoeology in High Mountain Environments. *Geogr. J.* **1996**, *164*, 218. [[CrossRef](#)]
5. Berthling, I. Beyond Confusion: Rock Glaciers as Cryo-Conditioned Landforms. *Geomorphology* **2011**, *131*, 98–106. [[CrossRef](#)]
6. Käab, A.; Strozzi, T.; Bolch, T.; Caduff, R.; Kon Trefall, H.; Stoffel, M.; Kokarev, A. Inventory and Changes of Rock Glacier Creep Speeds in Ile Alatau and Kungöy Ala-Too, Northern Tien Shan, since the 1950s. *Cryosphere* **2021**, *15*, 927–949. [[CrossRef](#)]
7. Barsch, D. Nature and importance of mass-wasting by rock glaciers in alpine permafrost environments. *Earth Surf. Process.* **1977**, *2*, 231–245. [[CrossRef](#)]
8. Humlum, O. The Geomorphic Significance of Rock Glaciers: Estimates of Rock Glacier Debris Volumes and Headwall Recession Rates in West Greenland. *Geomorphology* **2000**, *35*, 41–67. [[CrossRef](#)]
9. Brenning, A. Geomorphological, Hydrological and Climatic Significance of Rock Glaciers in the Andes of Central Chile (33–35°S). *Permafrost Periglac. Process.* **2005**, *16*, 231–240. [[CrossRef](#)]

10. Degenhardt, J.J. Development of Tongue-Shaped and Multilobate Rock Glaciers in Alpine Environments—Interpretations from Ground Penetrating Radar Surveys. *Geomorphology* **2009**, *109*, 94–107. [[CrossRef](#)]
11. *Towards Standard Guidelines for Inventorying Rock Glaciers: Baseline Concepts (Version 4.2.2)*; IPA Action Group Rock Glacier Inventories and Kinematics, 2022; pp. 1–13. Available online: https://bigweb.unifr.ch/Science/Geosciences/Geomorphology/Pub/Website/IPA/Guidelines/V4/220331_Baseline_Concepts_Inventorying_Rock_Glaciers_V4.2.2.pdf (accessed on 29 December 2022).
12. *Towards Standard Guidelines for Inventorying Rock Glaciers: Practical Concepts (Version 2.0)*; IPA Action Group Rock Glacier Inventories and Kinematics, 2022; pp. 1–10. Available online: https://bigweb.unifr.ch/Science/Geosciences/Geomorphology/Pub/Website/IPA/Guidelines/RGI_PC/V2/220411_Practical_Concepts_Inventorying_Rock_Glaciers_V2.0.pdf (accessed on 29 December 2022).
13. Jones, D.B.; Harrison, S.; Anderson, K.; Betts, R.A. Mountain Rock Glaciers Contain Globally Significant Water Stores. *Sci. Rep.* **2018**, *8*, 2834. [[CrossRef](#)]
14. Azócar, G.F.; Brenning, A. Hydrological and Geomorphological Significance of Rock Glaciers in the Dry Andes, Chile (27–33°s). *Permafrost Periglacial Process.* **2010**, *21*, 42–53. [[CrossRef](#)]
15. Rangecroft, S.; Harrison, S.; Anderson, K. Rock Glaciers as Water Stores in the Bolivian Andes: An Assessment of Their Hydrological Importance. *Arct. Antarct. Alp. Res.* **2015**, *47*, 89–98. [[CrossRef](#)]
16. Villarroel, C.D.; Beliveau, G.T.; Forte, A.P.; Monserrat, O.; Morvillo, M. DInSAR for a Regional Inventory of Active Rock Glaciers in the Dry Andes Mountains of Argentina and Chile with Sentinel-1 Data. *Remote Sens.* **2018**, *10*, 1588. [[CrossRef](#)]
17. Halla, C.; Henrik Blöthe, J.; Tapia Baldis, C.; Trombotto Liaudat, D.; Hilbich, C.; Hauck, C.; Schrott, L. Ice Content and Interannual Water Storage Changes of an Active Rock Glacier in the Dry Andes of Argentina. *Cryosphere* **2021**, *15*, 1187–1213. [[CrossRef](#)]
18. Millar, C.I.; Westfall, R.D.; Delany, D.L. Thermal and Hydrologic Attributes of Rock Glaciers and Periglacial Talus Landforms: Sierra Nevada, California, USA. *Quat. Int.* **2013**, *310*, 169–180. [[CrossRef](#)]
19. Anderson, R.S.; Anderson, L.S.; Armstrong, W.H.; Rossi, M.W.; Crump, S.E. Glaciation of Alpine Valleys: The Glacier—Debris-Covered Glacier—Rock Glacier Continuum. *Geomorphology* **2018**, *311*, 127–142. [[CrossRef](#)]
20. Brighenti, S.; Tolotti, M.; Bruno, M.C.; Wharton, G.; Pusch, M.T.; Bertoldi, W. Ecosystem Shifts in Alpine Streams under Glacier Retreat and Rock Glacier Thaw: A Review. *Sci. Total Environ.* **2019**, *675*, 542–559. [[CrossRef](#)] [[PubMed](#)]
21. Jones, D.B.; Harrison, S.; Anderson, K.; Whalley, W.B. Rock Glaciers and Mountain Hydrology: A Review. *Earth-Sci. Rev.* **2019**, *193*, 66–90. [[CrossRef](#)]
22. Ran, Z.; Liu, G. Rock Glaciers in Daxue Shan, South-Eastern Tibetan Plateau: An Inventory, Their Distribution, and Their Environmental Controls. *Cryosphere* **2018**, *12*, 2327–2340. [[CrossRef](#)]
23. Scotti, R.; Brardinoni, F.; Alberti, S.; Frattini, P.; Crosta, G.B. A Regional Inventory of Rock Glaciers and Protalus Ramparts in the Central Italian Alps. *Geomorphology* **2013**, *186*, 136–149. [[CrossRef](#)]
24. Humlum, O. The Climatic Significance of Rock Glaciers. *Permafrost Periglacial Process.* **1998**, *9*, 375–395. [[CrossRef](#)]
25. Konrad, S.K.; Humphrey, N.F.; Steig, E.J.; Clark, D.H.; Potter, N.; Pfeffer, W.T. Rock Glacier Dynamics and Paleoclimatic Implications. *Geology* **1999**, *27*, 1131–1134. [[CrossRef](#)]
26. Millar, C.I.; Westfall, R.D.; Evenden, A.; Holmquist, J.G.; Schmidt-Gengenbach, J.; Franklin, R.S.; Nachlinger, J.; Delany, D.L. Potential Climatic Refugia in Semi-Arid, Temperate Mountains: Plant and Arthropod Assemblages Associated with Rock Glaciers, Talus Slopes, and Their Forefield Wetlands, Sierra Nevada, California, USA. *Quat. Int.* **2015**, *387*, 106–121. [[CrossRef](#)]
27. Sorg, A.; Käab, A.; Roesch, A.; Bigler, C.; Stoffel, M. Contrasting Responses of Central Asian Rock Glaciers to Global Warming. *Sci. Rep.* **2015**, *5*, 8228. [[CrossRef](#)]
28. Rock Glacier Velocity as an associated parameter of ECV Permafrost (Version 3.1). IPA Action Group Rock glacier inventories and kinematics, 2022; 12p. Available online: https://bigweb.unifr.ch/Science/Geosciences/Geomorphology/Pub/Website/IPA/RGV/RockGlacierVelocity_V3.1.pdf (accessed on 29 December 2022).
29. Käab, A.; Frauenfelder, R.; Roer, I. On the Response of Rockglacier Creep to Surface Temperature Increase. *Glob. Planet. Chang.* **2007**, *56*, 172–187. [[CrossRef](#)]
30. Kellerer-Pirklbauer, A.; Kaufmann, V. About the Relationship between Rock Glacier Velocity and Climate Parameters in Central Austria. *Austrian J. Earth Sci.* **2012**, *105*, 94–112.
31. Kenner, R.; Pruessner, L.; Beutel, J.; Limpach, P.; Phillips, M. How Rock Glacier Hydrology, Deformation Velocities and Ground Temperatures Interact: Examples from the Swiss Alps. *Permafrost Periglacial Process.* **2020**, *31*, 3–14. [[CrossRef](#)]
32. Cicoira, A.; Beutel, J.; Faillietaz, J.; Vieli, A. Water Controls the Seasonal Rhythm of Rock Glacier Flow. *Earth Planet. Sci. Lett.* **2019**, *528*, 115844. [[CrossRef](#)]
33. Wirz, V.; Gruber, S.; Purves, R.S.; Beutel, J.; Gärtner-Roer, I.; Gubler, S.; Vieli, A. Short-Term Velocity Variations at Three Rock Glaciers and Their Relationship with Meteorological Conditions. *Earth Surf. Dyn.* **2016**, *4*, 103–123. [[CrossRef](#)]
34. Strozzi, T.; Caduff, R.; Jones, N.; Barboux, C.; Delaloye, R.; Bodin, X.; Käab, A.; Mätzler, E.; Schrott, L. Monitoring Rock Glacier Kinematics with Satellite Synthetic Aperture Radar. *Remote Sens.* **2020**, *12*, 559. [[CrossRef](#)]
35. Delaloye, R.; Barboux, C.; Bodin, X.; Brenning, A.; Hartl, L.; Hu, Y.; Ikeda, A.; Kaufmann, V.; Kellerer-Pirklbauer, A.; Lambiel, C.; et al. Rock Glacier Inventories and Kinematics: A New IPA Action Group. In Proceedings of the 5th European Conference on Permafrost, Chamonix-Mont Blanc, France, 23 June–1 July 2018; p. 18.
36. Barsch, D. Permafrost Creep and Rockglaciers. *Permafrost Periglacial Process.* **1992**, *3*, 175–188. [[CrossRef](#)]

37. Brardinoni, F.; Scotti, R.; Sailer, R.; Mair, V. Evaluating Sources of Uncertainty and Variability in Rock Glacier Inventories. *Earth Surf. Process. Landf.* **2019**, *44*, 2450–2466. [CrossRef]
38. Yague-Martinez, N.; Prats-Iraola, P.; Gonzalez, F.R.; Brcic, R.; Shau, R.; Geudtner, D.; Eineder, M.; Bamler, R. Interferometric Processing of Sentinel-1 TOPS Data. *IEEE Trans. Geosci. Remote Sens.* **2016**, *54*, 2220–2234. [CrossRef]
39. Necsoiu, M.; Onaca, A.; Wigginton, S.; Urdea, P. Rock Glacier Dynamics in Southern Carpathian Mountains from High-Resolution Optical and Multi-Temporal SAR Satellite Imagery. *Remote Sens. Environ.* **2016**, *177*, 21–36. [CrossRef]
40. Wang, X.; Liu, L.; Zhao, L.; Wu, T.; Li, Z.; Liu, G. Mapping and Inventorying Active Rock Glaciers in the Northern Tien Shan of China Using Satellite SAR Interferometry. *Cryosphere* **2017**, *11*, 997–1014. [CrossRef]
41. Brencher, G.; Handwerker, A.L.; Munroe, J.S. InSAR-Based Characterization of Rock Glacier Movement in the Uinta Mountains, Utah, USA. *Cryosphere* **2021**, *15*, 4823–4844. [CrossRef]
42. *Optional Kinematic Attribute in Standardized Rock Glacier Inventories (Version 3.0.1)*; IPA Action Group Rock Glacier Inventories and Kinematics, 2022. Available online: https://bigweb.unifr.ch/Science/Geosciences/Geomorphology/Pub/Website/IPA/CurrentVersion/Current_KinematicalAttribute.pdf (accessed on 29 December 2022).
43. Palgov, N. Glaciers of Bolshaja Almatinka in Zailiyskij Alatau. *News of the MGO*, 1 January 1932; 322–326. (In Russian)
44. Goloskokov, V. *Old Glaciers of Zailiyskij Alatau*; Academy of Sciences of the Kazakh SSR: Almaty, Kazakhstan, 1949; pp. 80–82. (In Russian)
45. Iveronova, M. *Rock Glaciers in Northern Tien Shan*; Institute of Geography of the Academy of Sciences of the USSR: Moscow, Russia, 1950; pp. 69–88. (In Russian)
46. Gorbunov, A. *Permafrost in Tien Shan*; Publishing house Ilim: Bishkek, Kyrgyzstan, 1967; pp. 1–164. (In Russian)
47. Gorbunov, A. *Rock Glaciers of Zailiyskij Alatau*; USSR Academy of Sciences: Moscow, Russia, 1979; pp. 5–34. (In Russian)
48. Gorbunov, A.; Titkov, S. *Rock Glaciers of the Central Asian Mountains*; USSR Academy of Sciences: Moscow, Russia, 1989; pp. 1–164. (In Russian)
49. Gorbunov, A.; Titkov, S.; Polyakov, V. Dynamics of Rock Glaciers of the Northern Tien Shan and the Djungar Ala Tau, Kazakhstan. *Permafrost Periglacial Process.* **1992**, *3*, 29–39. [CrossRef]
50. Palgov, N. Movement Observations of a Rock Glacier in the Dzhungar Alatau. *Quest. Geogr. Kazakhstan* **1957**, *2*, 195–207. (In Russian)
51. Vilesov, E.; Morozova, V.; Seversky, I. *Glaciation of the Dzungarian (Zhetysu) Alatau: Past, Present, Future*; KazNU: Almaty, Kazakhstan, 2013. (In Russian)
52. Yudichev, M. *Dzungarian Alatau. Materials on Geology and Minerals of Kazakhstan*; KazFAN USSR: Leningrad, Russia, 1940; Volume 14. (In Russian)
53. Gorbunov, A.; Gorbunova, I. *Geography of Rock Glaciers of the World*; KMK Scientific Press Ltd.: Moscow, Russia, 2010. (In Russian)
54. Kaldybayev, A.; Chen, Y.; Vilesov, E. Glacier Change in the Karatal River Basin, Zhetysu (Dzhungar) Alatau, Kazakhstan. *Ann. Glaciol.* **2016**, *57*, 11–19. [CrossRef]
55. Cherkasov, P. *Glacier Inventory of the USSR. Lake Balkhash Basin, Part 4*; Hydrometeorological Publishing House: Leningrad, Russia, 1975; Volume 13. (In Russian)
56. Cherkasov, P. *Glacier Inventory of the USSR. Lake Balkhash Basin, Part 5*; Hydrometeorological Publishing House: Leningrad, Russia, 1980; Volume 13. (In Russian)
57. Cherkasov, P. *Glacier Inventory of the USSR. Lake Balkhash Basin, Part 6*; Hydrometeorological Publishing House: Leningrad, Russia, 1970; Volume 13. (In Russian)
58. Cherkasov, P.; Erasov, V. *Glacier Inventory of the USSR. Lake Balkhash Basin, Part 7*; Hydrometeorological Publishing House: Leningrad, Russia, 1969; Volume 13. (In Russian)
59. Pieczonka, T.; Bolch, T. Region-Wide Glacier Mass Budgets and Area Changes for the Central Tien Shan between ~1975 and 1999 Using Hexagon KH-9 Imagery. *Glob. Planet. Chang.* **2015**, *128*, 1–13. [CrossRef]
60. Narama, C.; Kääh, A.; Duishonakunov, M.; Abdrakhmatov, K. Spatial Variability of Recent Glacier Area Changes in the Tien Shan Mountains, Central Asia, Using Corona (~1970), Landsat (~2000), and ALOS (~2007) Satellite Data. *Glob. Planet. Chang.* **2010**, *71*, 42–54. [CrossRef]
61. Severskiy, I.; Vilesov, E.; Armstrong, R.; Kokarev, A.; Kogutenko, L.; Usmanova, Z.; Morozova, V.; Raup, B. Changes in Glaciation of the Balkhash-Alakol Basin, Central Asia, over Recent Decades. *Ann. Glaciol.* **2016**, *57*, 382–394. [CrossRef]
62. Reinosch, E.; Gerke, M.; Riedel, B.; Schwalb, A.; Ye, Q.; Buckel, J. Rock Glacier Inventory of the Western Nyainqentanglha Range, Tibetan Plateau, Supported by InSAR Time Series and Automated Classification. *Permafrost Periglacial Process.* **2021**, *32*, 657–672. [CrossRef]
63. Liu, L.; Millar, C.I.; Westfall, R.D.; Zebker, H.A. Surface Motion of Active Rock Glaciers in the Sierra Nevada, California, USA: Inventory and a Case Study Using InSAR. *Cryosphere* **2013**, *7*, 1109–1119. [CrossRef]
64. Bertone, A.; Barboux, C.; Bodin, X.; Bolch, T.; Brardinoni, F.; Caduff, R.; Christiansen, H.H.; Darrow, M.M.; Delaloye, R.; Etzelmüller, B.; et al. Incorporating InSAR Kinematics into Rock Glacier Inventories: Insights from 11 Regions Worldwide. *Cryosphere* **2022**, *16*, 2769–2792. [CrossRef]
65. Stumm, D.; Schmid, M.-O.; Gruber, S.; Baral, P.; Shahi, S.; Shrestha, T.; Wester, P. *Manual for Mapping Rock Glaciers in Google Earth*; International Centre For Integrated Mountain Development (ICIMOD): Kathmandu, Nepal, 2015.

66. Pandey, P. Inventory of Rock Glaciers in Himachal Himalaya, India Using High-Resolution Google Earth Imagery. *Geomorphology* **2019**, *340*, 103–115. [[CrossRef](#)]
67. Butler, D. The Web-Wide World. *Nature* **2006**, *439*, 776–778. [[CrossRef](#)]
68. Nourbakhsh, I.; Sargent, R.; Wright, A.; Cramer, K.; McClendon, B.; Jones, M. Mapping Disaster Zones. *Nature* **2006**, *439*, 787–788. [[CrossRef](#)]
69. Ballagh, L.M.; Parsons, M.A.; Swick, R. Visualising Cryospheric Images in a Virtual Environment: Present Challenges and Future Implications. *Polar Rec.* **2007**, *43*, 305–310. [[CrossRef](#)]
70. Ballagh, L.M.; Raup, B.H.; Duerr, R.E.; Khalsa, S.J.S.; Helm, C.; Fowler, D.; Gupte, A. Representing Scientific Data Sets in KML: Methods and Challenges. *Comput. Geosci.* **2011**, *37*, 57–64. [[CrossRef](#)]
71. Chang, A.Y.; Parrales, M.E.; Jimenez, J.; Sobieszczyk, M.E.; Hammer, S.M.; Copenhaver, D.J.; Kulkarni, R.P. Combining Google Earth and GIS Mapping Technologies in a Dengue Surveillance System for Developing Countries. *Int. J. Health Geogr.* **2009**, *8*, 49. [[CrossRef](#)] [[PubMed](#)]
72. Sheppard, S.R.J.; Cizek, P. The Ethics of Google Earth: Crossing Thresholds from Spatial Data to Landscape Visualisation. *J. Environ. Manag.* **2009**, *90*, 2102–2117. [[CrossRef](#)]
73. Yu, L.; Gong, P. Google Earth as a Virtual Globe Tool for Earth Science Applications at the Global Scale: Progress and Perspectives. *Int. J. Remote Sens.* **2012**, *33*, 3966–3986. [[CrossRef](#)]
74. Schmid, M.O.; Baral, P.; Gruber, S.; Shahi, S.; Shrestha, T.; Stumm, D.; Wester, P. Assessment of Permafrost Distribution Maps in the Hindu Kush Himalayan Region Using Rock Glaciers Mapped in Google Earth. *Cryosphere* **2015**, *9*, 2089–2099. [[CrossRef](#)]
75. Charbonneau, A.A.; Smith, D.J. An Inventory of Rock Glaciers in the Central British Columbia Coast Mountains, Canada, from High Resolution Google Earth Imagery. *Arct. Antarct. Alp. Res.* **2018**, *50*, e1489026. [[CrossRef](#)]
76. Rangecroft, S.; Harrison, S.; Anderson, K.; Magrath, J.; Castel, A.P.; Pacheco, P. A First Rock Glacier Inventory for the Bolivian Andes. *Permafr. Periglac. Process.* **2014**, *25*, 333–343. [[CrossRef](#)]
77. Haeberli, W.; Hallet, B.; Arenson, L.; Elconin, R.; Humlum, O.; Kääh, A.; Kaufmann, V.; Ladanyi, B.; Matsuoka, N.; Springman, S.; et al. Permafrost Creep and Rock Glacier Dynamics. *Permafr. Periglac. Process.* **2006**, *17*, 189–214. [[CrossRef](#)]
78. Rosen, P.A. Synthetic Aperture Radar Interferometry. *Proc. IEEE* **2000**, *88*, 333–380. [[CrossRef](#)]
79. Klees, R.; Massonnet, D. Deformation Measurements Using SAR Interferometry: Potential and Limitations. *Geol. En Mijnb. /Neth. J. Geosci.* **1998**, *77*, 161–176. [[CrossRef](#)]
80. Berardino, P.; Fornaro, G.; Lanari, R.; Sansosti, E. A New Algorithm for Surface Deformation Monitoring Based on Small Baseline Differential SAR Interferograms. *IEEE Trans. Geosci. Remote Sens.* **2002**, *40*, 2375–2383. [[CrossRef](#)]
81. Sowter, A.; Bateson, L.; Strange, P.; Ambrose, K.; Fifiksiyafudin, M. Dinsar Estimation of Land Motion Using Intermittent Coherence with Application to the South Derbyshire and Leicestershire Coalfields. *Remote Sens. Lett.* **2013**, *4*, 979–987. [[CrossRef](#)]
82. Bateson, L.; Cigna, F.; Boon, D.; Sowter, A. The Application of the Intermittent SBAS (ISBAS) InSAR Method to the South Wales Coalfield, UK. *Int. J. Appl. Earth Obs. Geoinf.* **2015**, *34*, 249–257. [[CrossRef](#)]
83. *Rock Glacier Inventory Using InSAR (Kinematic Approach), Practical Guidelines (Version 3.0.2)*; IPA Action Group Rock Glacier Inventories and Kinematics, 2020. Available online: https://bigweb.unifr.ch/Science/Geosciences/Geomorphology/Pub/Website/CCI/CurrentVersion/Current_InSAR-based_Guidelines.pdf (accessed on 29 December 2022).
84. Kaldybayev, A.; Yaning, C. Assessment of changes in the area of glaciers in the northern part of the zhetysu alatau based on remote sensing data. *J. Geogr. Environ. Manag.* **2022**, *2022*, 4–16. [[CrossRef](#)]
85. Notti, D.; Herrera, G.; Bianchini, S.; Meisina, C.; García-Davalillo, J.C.; Zucca, F. A Methodology for Improving Landslide PSI Data Analysis. *Int. J. Remote Sens.* **2014**, *35*, 2186–2214. [[CrossRef](#)]
86. Cherkasov, P. Dynamics of a Low-Littered Rock Glacier in the Dzungarian Alatau for 35 Years. In *Glaciers, Snow Cover and Avalanches in the Mountains of Kazakhstan*; Publishing house Nauka: Alma-Ata, Kazakhstan, 1989; pp. 180–216. (In Russian)

Disclaimer/Publisher’s Note: The statements, opinions and data contained in all publications are solely those of the individual author(s) and contributor(s) and not of MDPI and/or the editor(s). MDPI and/or the editor(s) disclaim responsibility for any injury to people or property resulting from any ideas, methods, instructions or products referred to in the content.